CRACK GROWTH RESISTANCE AND FRACTURE TOUGHNESS ENHANCEMENT OF ALUMINA / ZIRCONIA FUNCTIONALLY GRADIENT MATERIAL

P. Hvizdoš, K. Norberg

Abstract

The effect of the residual stresses arising due to the thermal expansion mismatch between layers in an alumina/zirconia FGM on the crack growth behaviour has been studied. The residual stresses were measured by indentation method and calculated using an analytical model of symmetrical FGM structure. Macroscopic fracture toughness at room temperature has been investigated by studying the crack growth behaviour of indented specimens at various stress levels. The apparent R-curve for the cracks propagating within the compressive layers has been constructed. It was shown that the macroscopic compressive stresses present within the exterior layers significantly hindered the crack propagation and enhanced the apparent fracture toughness, which increased from 3 to 8.7 MPa.m$^{1/2}$, thus improving reliability of the FGM.

Keywords: FGM, alumina, zirconia, layered composites, electrophoretic deposition, residual stress, R-curve

INTRODUCTION

One of the possibilities for solving the problem of the sensitivity to flaws in ceramics is introducing toughening mechanisms using platelets, secondary particles, whiskers or fibres. Another well recognised method that has proven inexpensive, and is commonly used in glasses, is the introduction of surface compressive stresses, particularly when resistance to impact and surface damage is required. In ceramics this can be obtained by forming a laminate ceramic composite. In multilayered materials with strong interfaces the difference in the thermal expansion coefficients between dissimilar materials generate thermal residual stresses during subsequent cooling [1,2]. The relative thickness of different layers determines the relative magnitudes of stresses, while the magnitude of the strain mismatch between the layers implies the absolute values of the residual stresses. However, abrupt transitions in the composition and properties of these materials often result in sharp local concentrations of stress, whether the stress is internal or applied externally. This may lead to cracking of the interface during cooling from the processing temperature or to delamination in service. A possible solution is a concept of functionally graded materials (FGMs). Their main feature is a gradient in composition and/or phase distribution and related mechanical and physical properties. The controlled modifications of the composition can reduce the magnitude of the thermal stresses, suppress the plastic flow and cracking and improve interfacial bonding, provided that the graded microstructure is thermally stable during subsequent thermomechanical loading.

The aim of the present work is the study thermal residual stresses of a symmetrical planar alumina/zirconia FGM and their influence on the crack growth within the bulk of a

Pavol Hvizdoš, K. Norberg, Department of Materials, Universitat Politécnica de Catalunya, ETSEIB, Barcelona, Spain

FGM. The indentation crack growth was observed by means of bending tests and rising fracture toughness and was described in terms of R-curve.

MATERIAL

The material was an experimental grade manufactured by Katholieke Universiteit Leuven, Belgium, the details had been described previously in [3]. The starting materials were commercially available powders of 3 mol% Y_2O_3 co-precipitated ZrO_2 (Daiichi grade HSY-3U) with an average particle size ~0.3 mm and α-Al_2O_3 (Baikowski grade SM8) with an average particle size ~0.6 mm. As-received powders were ball-milled in ethanol for 24 hours. Electrophoretic deposition (EPD) at a constant voltage was performed in a suspension flow-through deposition cell, where a supply system adds a second suspension to the circulating suspension in the mixing cell at a controlled rate. The process was performed in a way that would in theory lead to a symmetrical configuration of the layered system. The green bodies obtained with the EPD were sintered for 2 h at 1500°C.

The resulting material was supplied in the form of discs approximately 4 mm thick and with a diameter of 36 mm. The two outer layers (0.7 mm thick) consisted of a homogeneous mixture of 90% Al_2O_3 and 10% ZrO_2, the inner layer (2 mm thick) was a homogeneous mixture of 70% Al_2O_3 with 30% ZrO_2. The graded interlayers were about 0.3 mm thick.

EXPERIMENTAL METHODS

Microstructure

In order to observe the microstructure of all layers of the experimental material, the discs were cut perpendicularly with respect to the layers, the cross section surfaces were polished and thermally etched (1200°C for 2 hours in ambient air). The microstructure features were then studied using a SEM with an attached EDS unit.

Indentation

Mechanical properties were investigated using indentation methods. Vickers hardness was measured across the polished surface of the specimen primarily in order to find the hardness profile using a standard hardness tester. In all cases the indents were aligned so that their diagonals and possible radial cracks were parallel and perpendicular to the composite layers. The sizes of the indents and the crack lengths were measured by an optical microscope. Indentation fracture toughness (K_{IC}) was calculated from the length of the cracks induced by the same indents using the Anstis [4] formula:

$$K_{IC} = \eta \, (E/H)^{1/2} \, F / c^{3/2} \qquad (1)$$

where η is a geometric factor estimated as 0.016, E is the modulus of elasticity, H is the hardness, F is the indentation load, and c is the indentation radial crack half-length at the surface. Here, the c values were the lengths of the cracks parallel to the layers only, because these were not influenced by the in-plane residual stresses. From the length difference between these cracks (c, unstressed) and the cracks perpendicular to the layers (c_R, stressed) the in-plane residual stress (σ_R) can be calculated [5]

$$\sigma_R = K_{IC} \, [1 - (c/c_R)^{3/2}] / (Y \, c_R^{1/2}) \qquad \begin{matrix} > 0 \text{ tensile} \\ < 0 \text{ compressive,} \end{matrix} \qquad (2)$$

where K_I is the stress intensity factor for stressed crack, Y is the geometric factor ~1.26.

The residual stresses were calculated also theoretically, using a model of symmetrical laminar FGM developed in [6].

THEORETICAL MODEL OF THE RESIDUAL STRESSES

When plates of dissimilar materials are bonded together without cracks or macroscopic defects along their interfaces, a state of biaxial loading exists away from the free edges. In absence of bending the materials undergo normal stresses only in the in-plane directions and are free of shear stresses or out-of-plane stresses. The formulas for bulk residual stresses in symmetrical multilayered laminates consisting of layers of two different types were developed by several authors [7,8] and are well known. In the case of FGMs, however, the influence of gradient layers has to be taken to account as well, which is usually done by finite element methods. Yet, for simple enough configurations it is possible to use also analytical approach.

Consider a layered symmetrical system consisting of two types of homogeneous materials, *a* and *b*, with gradient layers in between (Fig.1). Here too, no bending takes place and momenta cancel each other. Assuming that the gradient profile is linear, we apply the linear rule of mixture for all basic material characteristics. Further more, we assume that the suffered thermal strain is a function of *z* only [9].

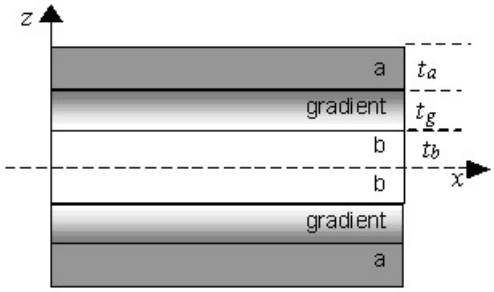

Fig.1. Schematic of symmetrical planar functionally graded material with layer thickness t_a, t_b, and t_g, respectively.

The bulk residual stresses within the homogeneous layers then can be calculated as:

$$\sigma_a = \Delta\varepsilon E'_a \frac{6E'_b t_b + (E'_a + 2E'_b)t_g}{6E'_a t_a + 6E'_b t_b + (3E'_a + 3E'_b)t_g}$$

$$\sigma_b = -\Delta\varepsilon E'_b \frac{6E'_a t_a + (2E'_a + E'_b)t_g}{6E'_a t_a + 6E'_b t_b + (3E'_a + 3E'_b)t_g} \qquad (3)$$

where E' is the biaxial modulus calculated as $E'=E/(1-\nu)$ from Young's modulus E and Poisson's ratio ν, and

$$\Delta\varepsilon = \int_T (\alpha_a - \alpha_b)dT \qquad (4)$$

is the thermal strain mismatch, calculated from the difference between thermal expansion coefficients α. The subscripts *a* and *b* denote the respective materials.

The consequences of the model for the design of the residual stresses in FGMs are discussed in detail in [6].

Crack propagation

The crack propagation was studied by 4-point bending tests of indented specimen (indentation fracture). Two types of bending bars were prepared from the primary discs, with different polished and indented tensile surfaces: type S – the tensile surface is identical to the original FGM surface, and type C – the tensile surface is a cross section of the material (Fig.2). The dimensions of the bars were 5x5x32 mm. The indents in the C-bar were placed in two lines, one in the inner layer, the other in the outer one. The experiments were carried out using universal testing machine Instron 8511 with spans of 10/20 mm (Fig.3). The total stress intensity factor (K_{tot}) was calculated as a sum of the part coming from indentation (K_{IC}) and that from the flexion (K_{app}) by bending stress σ:

$$K_{tot} = K_{IC} + K_{app} = \eta\,(E/H)^{1/2}\,F / c^{3/2} + Y\,\sigma\,c^{1/2} \qquad (5).$$

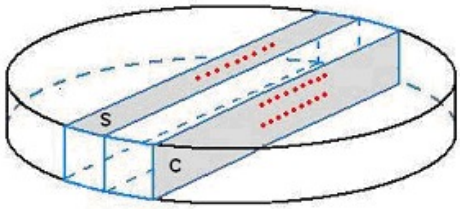

Fig.2. Schematic view of indented bars S (surface) and C (cross section).

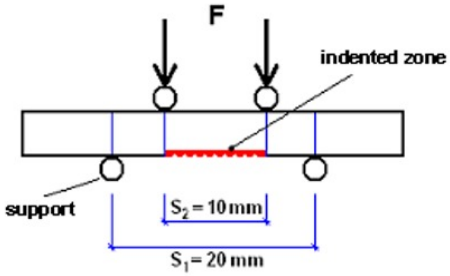

Fig.3. Schematic of 4-point bending test.

RESULTS

Microstructure

The microstructure studies of the experimental material have been presented elsewhere, [10]. Generally, the microstructure was well formed throughout the whole material (Fig.4). In the central layer (Fig.4a) it consisted of equiaxed alumina matrix grains with an average size of 0.5 – 0.9 μm and smaller homogeneously distributed zirconia grains with sizes between 0.2 μm and 0.4 μm. The zirconia grain clusters reached sizes up to 8 μm. The presence of zirconia effectively inhibited the alumina grain growth which can be demonstrated by the fact that in the outer layers with lower zirconia contents the alumina grains had typically sizes from 0.7 μm up to 1.5 μm (Fig.4b). In all layers only very little porosity was observed, and even this seemed to be mostly due to the grain pull-out during polishing rather than a real feature of the microstructure.

Concerning the layered structure, the outer homogeneous layers were 0.7 mm thick, the gradient ones 0.3 mm. The thickness of the inner homogeneous layer was 2 mm.

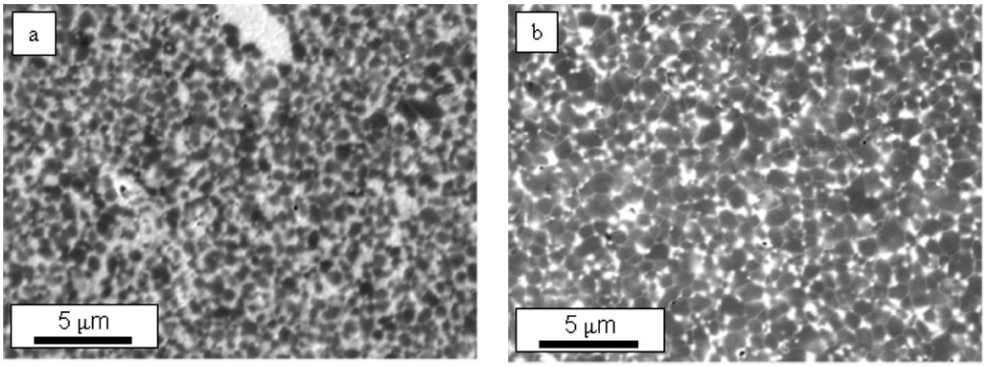

Fig.4. Microstructure of the homogeneous layers of the experimental material. (a) Central layer; (b) outer layer.

Mechanical properties

The mechanical properties are summarized in Table 1. As expected, results show that the exterior (surface) is harder than interior due to higher alumina content. The values even correspond to those of pure high quality alumina, and seem to be highly impact resistant. The detailed discussion of these results can be found in [10]. The calculated values are considerably higher than the measured ones, mainly due to the relaxation at the free surface.

Tab.1. Mechanical properties of the homogeneous layers in the FGM.

	Exterior (10% ZrO_2)	Interior (30% ZrO_2)
Hardness [GPa]	18.0 ± 1.5	17.0 ± 1.0
Fracture toughness [MPa.m$^{1/2}$]	3.5 ± 1	8.0 ± 0.5
Residual stress – measured [MPa]	- 270 ± 35 (compression)	110 ± 60 (tension)
Residual stress – calculated [MPa]	- 500 (compression)	352 (tension)

Crack propagation under applied bending loads

The measured fracture toughness (3.5 MPa.m$^{1/2}$) does not seem to be improved with respect to conventional composite with corresponding composition (~4.5 MPa.m$^{1/2}$ [11]). This is because at the surface the residual compressive stresses have relaxed. However, the situation changes when the cracks propagate into the bulk of the outer (compressive) layer. The graph on Fig.5 shows the apparent K_{tot} as a function of the crack length. This behaviour was studied observing mainly the 10 kg indentation cracks, as the rest of cracks were too short and the crack growth was not always clearly recognizable. It can be seen that the K_{tot} increases dramatically in the layer with the residual compressive stress, as the crack propagates through the layer. Again, the extrapolation of the results from sample S (surface) shows that the tendency is equivalent to that found in the exterior layer in sample C (cross section) for lower stresses. In these layers, the K_{tot} increases rapidly from ~3 MPa.m$^{1/2}$, which corresponds to the initial short cracks up to approximately

8.7 MPa.m$^{1/2}$ while the cracks grew up to 100% of their original length before the onset of the catastrophic failure of one of them. In contrast to that, in the central layer subjected to applied tension, the initial cracks grew very rapidly (elongation up to 300% of their original length) and reached the critical conditions at loads and stresses of only about one third (bending stress of 70 MPa) of those survived by the cracks in the compressive layers (203 MPa).

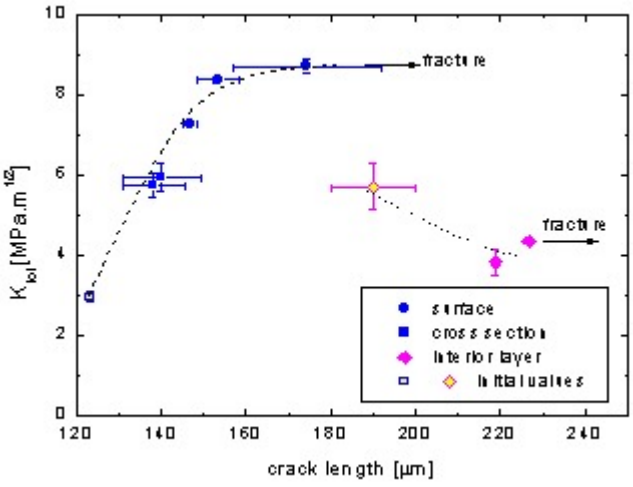

Fig.5. Total stress intensity factor (K_{tot}) vs crack length in four-point bending load tests.

This means that the outer layer exhibited strong positive R-curve effect, i.e. increase of the crack growth resistance with increasing crack length. As a consequence, the material would have a highly improved tolerance to (small) surface defects, whether technological ones or those produced during application (e.g. impact, scratching, etc).

In the central layer an opposite tendency, i.e. decrease of the K_{tot} with crack growth can be observed. This negative R-curve effect is caused by the present residual tensions.

Microscopic study of the crack paths showed that fracture micromechanisms were essentially the same in all stages of the crack growth (Fig.6). The very fine grained microstructure does not lead to crack deflection or bridging. Also, the role of the ZrO_2 phase transformation, if it occurs, is only secondary due to very small size of the ZrO_2 grains and their dispersion (volume fraction of 10%) within the matrix of the outer layer. This means that the present R-curve like behaviour is a macroscopic effect caused mainly by the layered structure, it is the so-called laminate toughening [1].

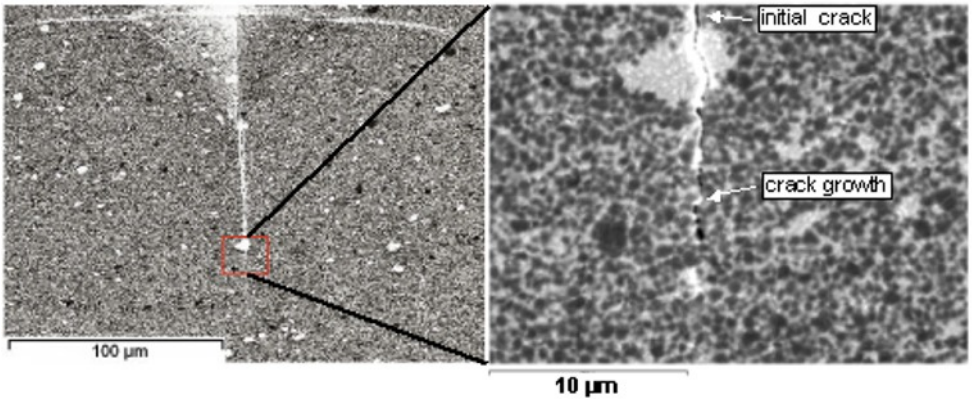

Fig.6. Micromechanisms of crack growth. Character of the initial indentation crack and the slow crack growth path, although the latter is more intergranular, is very similar. Even occasional clusters of zirconia grains (light coloured) do not change it significantly.

CONCLUSIONS

An experimental alumina/zirconia planar FGM prepared by EPD has been studied. The material had in all layers a high quality fine grained microstructure with very little overall porosity and uniformly distributed ZrO_2 within the homogeneous layers. The zirconia grains effectively hindered the growth of alumina matrix grains.

The hardness, fracture toughness, and residual stresses were measured by indentation methods on the cross-section of the sample. Their changes with respect to the compositional profile were identified. The material exhibited excellent hardness in the exterior layers, comparable to that of pure alumina.

The measured values of the residual stresses were compared to those calculated. The theoretical values tend to overestimate the results, mainly due to the free surface effect.

The study of indentation crack growth resistance showed in the outer layers a significant increase of apparent fracture toughness with an increasing transversal crack size – R-curve (from 3 up to 8.7 $MPa.m^{1/2}$).

No crack deviation at the layer interfaces and no delamination between the layers was observed, which is an effect of gradual changes of the stress states on the layer interfaces.

The experiments illustrate that suitable design and architecture of the layers with tailored residual stresses can result in enhanced defect tolerance and impact resistance of ceramic material.

Acknowledgements

The stay of PH at UPC was financed by the Spanish Ministry de Science and Technology via the "Ramón y Cajal" programme. The experimental materials were produced by Omer van Der Biest of KU Leuven, Belgium.

REFERENCES

[1] Lugovy, M., Orlovskaya, N., Berroth, K., Kuebler, J.: Composites Science and Technology, vol.59, 1999, p. 1429

[2] Suresh, S., Mortensen, A.: Fundamentals of functionally graded materials. Cambridge : ASM International and The Institute of Materials, 1995

[3] Vleugels, J., Anné, G., Put, S., Van Der Biest, O. In: Functionally Graded Materials VII. Trans Tech Publications, Switzerland, 2003, p. 171
[4] Anstis, GR., Chantikul, P., Lawn, BR., Marshall, DB.: J. Amer. Ceram. Soc., vol. 64, 1981, p. 533
[5] Green, DJ., Cai, PZ., Messing, GL.: J. Europ. Ceram. Soc., vol 19, 1999, p. 2511
[6] Hvizdoš, P., Norberg, K.: Key Engineering Materials, vol. 333, 2007, p. 259
[7] Virkar, AV., Huang, JL., Cutler, RA.: J. Amer. Ceram. Soc., vol. 70, 1987, p. 164
[8] Chartier, T., Merle, D., Besson, JL: J. Europ. Ceram. Soc., vol. 15, 1995, p. 101
[9] Giannakopoulos, AE., Suresh, S., Finot, M., Olsson, M.: Acta Metall. Mater., vol. 43, 1995, p. 1335
[10] Hvizdoš, P., Jonsson, D., Anglada, M., Anné, G., Van Der Biest, O.: J. Europ. Ceram. Society, vol. 27, 2007, p. 1365
[11] Casellas, D., Nagl, MM., Llanes, L., Anglada, M.: J. Materials Proc. Technology, vol. 143-144, 2003, p.148